

Engineering of materials for Solid Oxide Fuel Cells and other energy and environmental applications

Juan Carlos Ruiz-Morales,^{*a} David Marrero-López,^b Jesús Canales-Vázquez,^c Cristian Savaniu^d and Stanislav N. Savvin,^a

⁵ Received (in XXX, XXX) Xth XXXXXXXXXX 200X, Accepted Xth XXXXXXXXXX 200X

First published on the web Xth XXXXXXXXXX 200X

DOI: 10.1039/b000000x

The search of cleaner environmentally-friendly power sources has been the focus of the researchers' attention in the past few years. One of the most promising options for the production of clean energy is the Solid Oxide Fuel Cells and one of the simplest routes to improve the efficiency of these devices is the microstructural engineering of the component materials. In this work an insight into several cost-effective procedures of microstructural control of SOFC materials, ranging from "eye-scale" down to the micrometer scale, is provided. The proposed procedures may be considered general and as such they can be used to optimise various materials for energy and environmental-related areas.

Introduction

The climate change, the shortage of fossil fuels and the sharp increase in the energy demand, boosted mainly by some rising economies have led to a growing interest in the search of new and efficient ways of power generation. Furthermore, the power production in the World is currently based on combustion of fossil fuels, which makes even worse all the problems related to the quality of the air and the global warming effects (due to excessive production of CO₂). Fuel cells¹⁻³ appear to be an excellent alternative to most of the future power generation scenarios, in terms of low CO₂ emissions, quietness, site and fuel flexibility and power quality. Traditionally, a conventional route to improve the performance and durability of the state-of-the-art energy conversion and generation systems consisted in research of novel materials exhibiting outstanding properties. Recently it has been reported that integration of micro- and nanostructured materials may be considered an adequate strategy to achieve the goal.⁴

implants,⁵ design and fabrication of support materials for biofiltration,⁶ production of biofuels,⁷ design of materials for Solid Oxide Fuel Cell and enhancement of their performance,⁸⁻¹⁰ improvement of TiO₂-based photoelectrodes for Solar Cells,¹¹ development of TiO₂-based catalysts for the wastewaters treatments,¹² gas-separation membranes stable at high temperatures,¹³ nanomaterials for hydrogen storage,¹⁴ advanced heterogeneous catalysts,¹⁵ microstructural design of exhaust catalyst materials,¹⁶ Li-batteries,^{4,17} etc.

Solid Oxide Fuel Cells (SOFCs) are solid-state devices that produce electricity from the electrochemical combination of a fuel and an oxidant such as oxygen from air, water being the only by-product when hydrogen is used as fuel. Each single cell consist of two electrodes, an anode and a cathode, separated by a solid electrolyte, **Fig. 1**. These devices usually operate at elevated temperatures ranging between 800 and 1000 °C. The standard choice as electrolyte material is 8% yttria-stabilised zirconia (YSZ), strontium-substituted manganites such as La_{0.8}Sr_{0.2}MnO_{3-δ} (LSM) as cathodes whilst the state-of-the-art anode material is the Ni-YSZ cermet, **Fig. 1**.

There is a strong tendency to decrease the SOFC operating temperature, below 800 °C, which would give benefits in terms of choice and durability of materials (i.e. cheaper stainless steel interconnects). Moreover, lower temperatures would also release the constraints imposed by the cell components and seals. On the other hand, when the operating temperature decreases, the ohmic contribution of the YSZ electrolyte to the total electrical resistance of the cell becomes too high. This fact has led to the use of thinner electrolytes in anode-supported configurations or alternative electrolytes,³ with superior to that of YSZ, such as: Ce_{0.8}Gd_{0.2}O_{2-δ} (CGO),^{18,19} Ce_{0.8}Sm_{0.2}O_{2-δ} (CSO),^{18,19} La₂Mo₂O₉ (LAMO),²⁰⁻²² La_{0.9}Sr_{0.1}Ga_{0.8}Mg_{0.2}O_{2.85} (LSGM),²³ and apatite-type silicates.²⁴⁻²⁷

Regarding the anode, the widely used Ni-YSZ exhibits excellent catalytic properties, mixed conductivity and good current collecting properties, but low tolerance to sulphur,

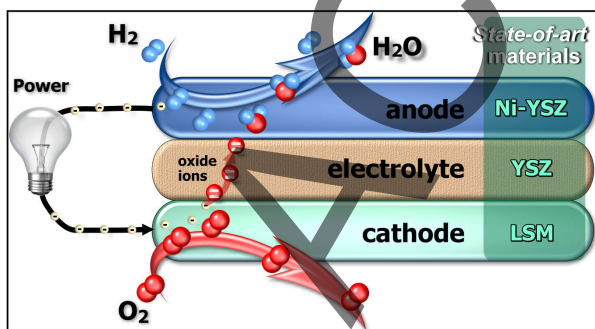


Fig. 1 Simple scheme of a SOFC, with the state-of-the-art materials used as anode, cathode and electrolyte.

This microstructural control has proven to be important not only in energy related fields but also in other relevant areas such as: control of the porosity and structure of ceramic bone

carbon build-up when exposed to hydrocarbon fuels and volume instability upon redox cycling.¹ Due to these problems and the fact that the anode material could effectively increase its efficiency working directly with hydrocarbon feed and therefore would not require the use of the external -and expensive- reformers, there have been done a lot of research addressing these issues.

Apart from the studies in alternatives cermet to the traditional Ni-YSZ, such as those based on Cu-ceria composites,^{28,29} ABO₃ perovskite oxides have been widely studied in the search for novel SOFC anodes. Indeed, some of the most relevant alternative anodes suggested in the past few years belong to this type of structural-type including mixed chromates-manganites,^{30,31} titanates^{8,32-35} and double perovskites as Sr₂MgMoO_{6-δ}.^{36,37}

Among perovskites, non-stoichiometric titanates with nominal oxygen excess are of especial interest due to their very high electronic conductivity, stability under reducing conditions and resistance to sulphur poisoning.³⁸⁻⁴¹ In particular, the studies by Canales-Vázquez *et al.*⁴¹ have shown that lanthanum strontium titanates chemically modified by introduction of Ga and Mn in the B-site render OCV voltages above 1.2 V and rather low polarisation resistances in methane.⁸ The outstanding properties of this system are due to a careful control of the structure at the nanometer scale, i.e. disrupting extended ordered defects by modifying the oxygen stoichiometry in the material, and further functionalisation via modification of the chemical composition,⁴¹ Fig. 2. This approach leads to promising performances as high as 0.5 W cm⁻² in pure hydrogen and over 0.3 W cm⁻² under humidified pure methane at 950 °C.⁸

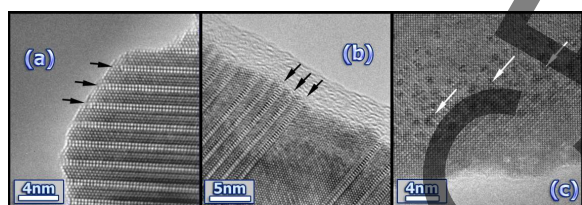


Fig. 2 HRTEM images of several members of the $\text{La}_4\text{Sr}_{n-4}\text{Ti}_{n-2}\text{O}_{3n-2}$ series where the structure varies from ordered extended planar oxygen excess defects (a), $n = 6$, through random layers of extended defects (b), $n = 8$, to disordered local defects (c), $n = 12$.⁸

Recently,⁴² it has been shown that some of these titanates ($\text{La}_4\text{Sr}_8\text{Ti}_{12}\text{O}_{38-\delta}$) may find use as catalysts of partial oxidation of methane to syngas yielding 88% CO and 89% H₂ selectivity at 30% CH₄ conversion. Hence, this material can be used to fabricate a dense ceramic membrane and become an alternative to the established industrial process of non-catalytic partial oxidation of methane to syngas, which typically requires very high temperature and high pressures.⁴³

On the other hand and as mentioned above, lowering the operating temperature to the intermediate temperature range (500-700 °C) has become one of the main priorities in the field of SOFCs. In this temperature range, the cathode polarisation makes significant contribution to the overall cell efficiency loss resulting from the high activation energy associated with the oxygen reduction reaction at the cathode

side. Whilst new cathodes based on simple perovskite-type mixed ionic-electronic conductors (MIECs) such as doped LaCoO₃, BaCoO₃ and LaFeO₃ have been extensively studied,⁴⁴⁻⁴⁷ not much attention has been paid to related structures such as double or layered perovskites. This may be due to the common belief that good cathodes should belong to simple structural types allowing three dimensional conduction pathways, particularly for oxide ion transport. However, several recent studies suggest the potential use of layered structures such as Ruddlesden-Popper, e.g. La₂NiO_{4+δ},⁴⁸⁻⁵⁰ or the classical layered high-temperature cuprate superconductor (YBa₂Cu₃O_{7-x}),⁵¹ as alternative SOFC cathodes. According to these studies, materials with layered structure as PrBaCo₂O_{5+x} (PBCO) or GdBaCo₂O_{5+x} (GBCO),⁵²⁻⁵⁵ show lower activation energy for the oxygen reduction, which converts them into suitable candidates for operation at reduced temperatures.

Hence, production of highly efficient fuel cells operating at the lowest possible temperature would be possible if some of the traditional SOFC components could be replaced by novel materials with special electrochemical properties and/or optimising if the microstructure of the corresponding components could be optimised to enhance the overall SOFC performance.

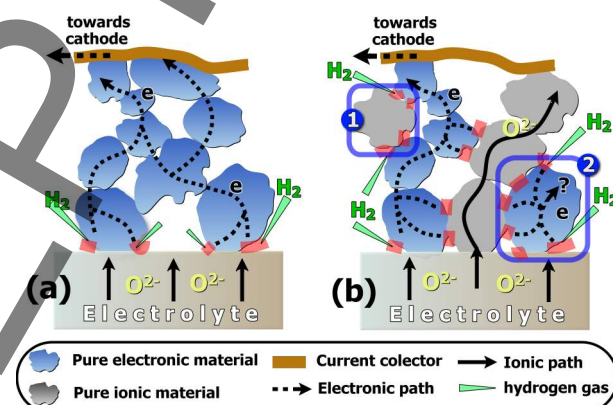


Fig. 3 Representations of Triple Phase Boundary (TPB) zones in (a) a pure electronic conductor in contact with an electrolyte. TPBs, in red colour, showing the movement of oxygen ions in the electrolyte toward the TPBs, which is limited to the electrolyte-electrode interface; and the movement of the electrons, produced in the TPBs, towards the current collector. (b) In a cermet material (with a metal and a pure ionic conductor), some potential TPB places may be deactivated because either there is not oxygen pathway toward the TPBs in (1); or the electrons (2) can not reach the current collector.

Nevertheless, the enhancement of the performance may also be achieved via the extension of the so-called Triple Phase Boundary (TPB). The TPB is the active area where the three phases necessary for the aforementioned electrochemical reactions meet: ion conducting phase, electron conducting phase, and gas phase, Fig. 3. The hydrogen gas in those TPBs produces protons and electrons. The electrons will move through the electronic material toward the current collector, where they will be used, in the cathode side, in the oxygen reduction producing oxygen ions. These ones will move through the electrolyte reaching the TPB zones in the anode, where they finally will react with the protons producing water. In a simple metal-based anode, Fig. 3(a), the TPB zone is just

restrited to the electrolyte-electrode interface and hence the performances abated are poor. Mixing and metal material with an pure ionic conductor will extend the TPB places through the electrode material, Fig. 3(b). However, to be really effective, all the TPB zones need to be connected to the electrolyte (ionic conduction paths) and to the current collector (electronic conduction paths). If any of them is missing, Fig. 3(b), then some TPB zones will not be really electrochemically active and SOFC device will be perform at lower efficiency. A simple solution to this problem is to use MIECs instead to use pure ionic conductors, and the alternative one is to achieve better control of the electrode microstructure that may certainly improve its performance.

Indeed, the effect of the electrode microstructure on the performance has been the subject of several articles such as those by Suzuki *et al.*⁹ and Zhang *et al.*,⁵⁶ not only in terms of electrochemical activity but also regarding mechanical stability of the fuel cell structure especially in electrode-supported configuration; optimisation of gases flow-paths to/from the reaction sites to minimise the concentration polarisation and hence avoiding extra ohmic contributions from contact grains and thermal instability and redox cycling.

The common route to control the porosity of these materials involves the use of pore formers, which generally are organic compounds that render a porous structure with undefined geometry after the corresponding thermal treatment.

Nowadays new procedures are proposed to precisely control the desired microstructural features of the electrode materials, e.g. type and distribution of the porosity, specific patterning, control of the layer thickness, incorporation of nanotubes to improve catalytic parameters, etc.

Herein we review the use of recently developed cost-effective methodologies, some of which are based on traditional processing routes,⁵⁷ that may be used for SOFC component development. Their applicability in other energy and environmental applications will also be briefly discussed.

1. Electrode/electrolyte impregnations

As mentioned before, the most convenient procedure to introduce porosity in SOFC electrodes is the use of pore formers, usually organic materials such as starch, graphite powder, glycine, polymers, etc. After the firing process, typically in excess of oxygen, the organic material is burnt off leaving behind a porous structure. This process does not allow control over the morphology of the porosity and hence the isolated TPB zones as those shown in Fig. 3(b) are more likely to be produced. An approach that has been explored so far is the production of porous structures that can be impregnated with nanoparticles of an adequate material, depending on the property to be introduced. A large number of articles dealing with this procedure has been published up to the date and here just a few examples will be shown. However, the excellent review of S. P. Jiang⁵⁸ is recommended to those interested in a more detailed description of this method.

To illustrate the effect of impregnations by oxide nanoparticles, it is worth mentioning that the performance of LSM cathode, which is rather poor at low temperatures, can

be improved by impregnation with cobaltite-ferrites.⁵⁹ Xu *et al.*⁶⁰ proposed a similar approach but using a SDC-based solution. Chen *et al.*⁶¹ were able to activate a porous YSZ backbone by impregnation with a cobaltite-ferrite to be used as cathode. The impregnation of catalyst materials such as palladium, typically used to improve the anode response,⁶² can also be used to improve the cathode response, Fig. 4.⁶³ In all cases, the key step is a firing treatment, at very low temperature (<600 °C), that allows the formation of functional nanoparticles. These nanoparticles can work as "contact points" between isolated TPBs, Fig. 3(b), thus enhancing the fuel cell performance, and/or they may act as a catalyst functional layer improving the kinetics of the reactions (towards the oxygen reduction in the cathode or the fuel oxidation in the anode).

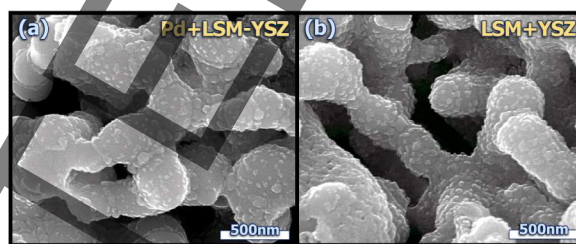


Fig. 4 Scanning electron micrographs of impregnations of Pd and LSM impregnated into a YSZ backbone. Reproduced from ref. 63 with permission.

2. Organic materials as pore formers

Using organic particles with some specific shape, e.g. microspheres will render a material with controlled porosity that can be directly related to the shape of the organic material.⁶⁴ The route is very simple and consists in the combination of nanometric oxide powders, a binder material and microspheres as pore formers such as polymethylmethacrylate (PMMA). The average size of the microspheres and their size distribution is determined by a careful control of the reaction conditions (temperature, stirring, initiator, etc.).⁶⁵ The optimisation of these conditions will allow obtaining spherical particles of uniform size and hence the porosity of the target material can be totally controlled. This method has been successfully used to improve the performance of SOFC materials⁵⁶ by up to 30%.⁶⁴

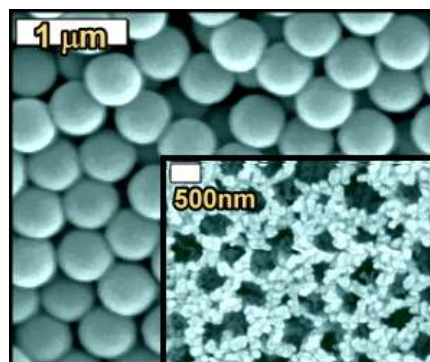


Fig. 5 SEM micrographs of PMMA microspheres of ~500 nm. The inset shows a sample of yttria stabilised zirconia (YSZ), prepared using YSZ and PMMA microspheres.⁶⁴

However, the main disadvantage is that the particle size of the starting oxide powders should be in the nanometric size range, which is not feasible for all materials. Furthermore, the high firing temperatures required to ensure an adequate contact between particles causes a significant decrease in the specific surface area of the final material due to particle agglomeration and sintering.

Savaniu *et al.*⁶⁶ reported the use of 200-500 nm PMMA microspheres as pore former to control the porosity of a La-doped SrTiO_3 ($\text{La}_x\text{Sr}_{1-3x/2}\text{TiO}_3$) as anode/(anode current collector) for intermediate temperature fuel cells. The anode support was prepared by aqueous tape casting. The button fuel cells ($\sim 2.5 \text{ cm}^2$ active area) were prepared by co-sintering the titanate substrate, YSZ electrolyte (75 μm of thickness) and a porous YSZ layer at 1400 $^\circ\text{C}$; the titanate was then pre-reduced at 1100 $^\circ\text{C}$ and impregnated by the solution of precursor of 20 mol% Gd-doped CeO_2 and Cu. A $\text{La}_{0.6}\text{Sr}_{0.4}\text{CoO}_3$ cathode was also prepared by impregnation into the porous YSZ backbone and in situ firing before measurement. Although relatively thick YSZ electrolyte has been used, power density superior to 0.5 W cm^{-2} has been obtained at 750 $^\circ\text{C}$, using pure humidified hydrogen and oxygen as fuel and oxidant respectively. This example demonstrates that a promising, robust ceramic anode for low temperature fuel cells can be created by combining electrode morphological design, pre-conditioning (i.e. reducing) and catalyst impregnation.

Another use of organic microspheres has been proposed by Brown *et al.*⁶⁷ In this case, a monolayer of polystyrene (PS) microspheres is deposited over an electrolyte. An oxygen plasma etching (OEP) allows reducing the size of the deposited microspheres. A thin metallic layer (Au, Pt or Ni) is then deposited by thermal evaporation, covering the gaps between the reduced microspheres generated by OEP and, finally, the organic material is removed, leaving behind a thin porous layer of metal covering the electrolyte. This layer exhibits highly reproducible features and hence the process may be interesting for mechanistic/modelling studies of metal-based fuel cell electrodes.

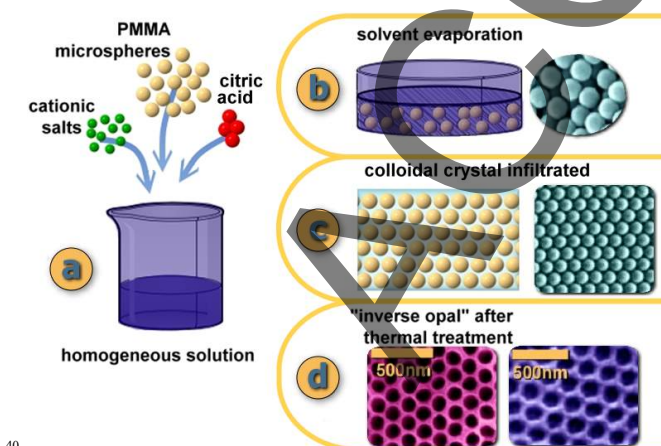


Fig. 6 (a) PMMA microspheres are dispersed in an aqueous solution of metal nitrates and citric acid. (b) The solution is left to dry slowly giving rise to a (c) infiltrated colloidal crystal. (d) A slow firing process to 600 $^\circ\text{C}$ and dwelling at this temperature for 5 h under air allows the

fabrication of an inorganic macroporous material with a 3D-ordered arrangement.

3. "Colloidal crystals" as templating materials

Porous materials with high surface area can also be obtained by using a colloidal crystal templating method.⁶⁹⁻⁷⁴ In this route, microspheres of organic materials are packed in an ordered arrangement, known as "colloidal crystal", **Fig. 6**. Such 3D matrix is then used as a template to infiltrate a solution containing the electrode and/or the catalyst material, in stoichiometric proportions, and afterwards the organic frame is removed by an appropriate thermal treatment, leaving a structure which is the negative of the colloidal crystal.

The precursor materials typically involve the use of expensive alkoxides for the production of simple oxides such as SiO_2 , TiO_2 , Al_2O_3 , which are the most common materials to be templated. Although complex systems such as $\text{La}_{1-x}\text{Sr}_x\text{FeO}_3$ has been also reported by Sadakane *et al.*⁷⁵

A economical way to produce similar structures involve the use of oxalic acid and metal nitrates to form the corresponding metal acetates.⁷⁶ A similar alternative method was proposed in 2008 by Marrero-López *et al.*⁷⁷ by introducing citric acid as complexing agent, **Fig. 6**, which allows the fabrication of 3D ordered macroporous layers of complex oxide materials such as YSZ, CGO, LAMOX, LSM, $\text{La}_{0.7}\text{Sr}_{0.3}\text{FeO}_{3-\delta}$ (LSF) $\text{La}_4\text{Sr}_8\text{Ti}_{11}\text{Mn}_{0.5}\text{Ga}_{0.5}\text{O}_{38-\delta}$ (LSTMG) and NiO-YSZ anodes, **Fig. 7**. These materials have been produced after firing between 450-650 $^\circ\text{C}$, rendering structures with 50% of porosity and relative high BET surface areas 11-38 m^2/g . However, the ordered areas are restricted to a few millimetres due to cracks produced during the shrinkage of the structure after removing the organic materials. In some cases, the microstructure is very likely to collapse during fabrication or even in operation conditions in a SOFC, at intermediate temperatures, due to the particle growth.

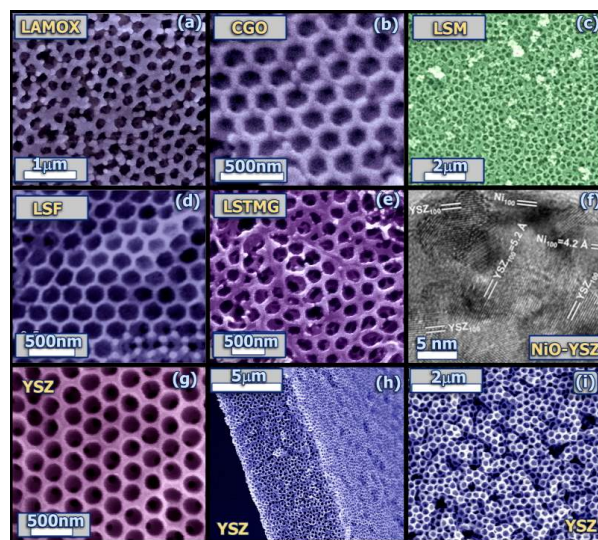


Fig. 7 Scanning electron micrographs of templated complex oxides systems using colloidal crystal of PMMA microspheres. (a) $\text{La}_2\text{Mo}_2\text{O}_9$ -electrolyte-, (b) $\text{Ce}_{0.8}\text{Gd}_{0.2}\text{O}_{2-\delta}$ -electrolyte-, (c) $\text{La}_{0.8}\text{Sr}_{0.2}\text{MnO}_{3-\delta}$ -cathode-, (d) $\text{La}_{0.7}\text{Sr}_{0.3}\text{FeO}_{3-\delta}$ -cathode-, (e) $\text{La}_4\text{Sr}_8\text{Ti}_{11}\text{Mn}_{0.5}\text{Ga}_{0.5}\text{O}_{38-\delta}$ -anode-, (f) NiO-YSZ -anode-, (g,h,i) YSZ -electrolyte-.

Lashtabeg *et al.*^{78,79} reported the successful production of the ordered YSZ-based structures even at 1400 °C, **Fig. 8**, using PS microspheres were used as the templating agent.

Lashtabeg *et al.* have shown that the firing temperature and the ratio organic-microspheres:inorganic-powder (OM:IP) are crucial for the mechanical stability of the microstructure and the BET surface area. The higher the firing temperature, the lower the BET surface area, e.g. increasing the firing temperature from 1000 °C to 1200 °C, with the same ratio, i.e. OM:IP=2:1, led to reduction of the BET surface in one order of magnitude. On the other hand, the higher the ratio OM:IP the lower the mechanical stability will be, the structure being more prone to partial collapsing.⁷⁸ Similar results have been reported by An *et al.*⁸⁰ for the creation of 3D-ordered thin layers of 8YSZ using PS templates.

This method of fabrication of materials with controlled porosity is really promising; however one important point must be addressed. The material produced has to be integrated in a SOFC, and therefore should be fixed to an electrolyte which is a very relevant issue. One may wonder how to co-fire the porous material to the dense layer corresponding to the electrolyte, avoiding any type of cracks.

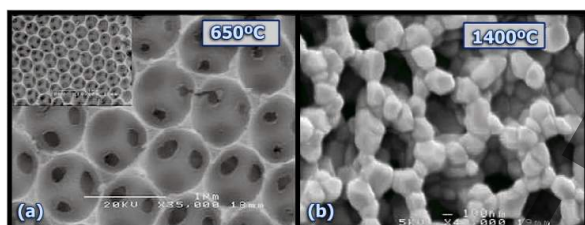


Fig. 8 Templated 4YSZ sintered at (a) 650 °C and (b) 1400 °C showing a regular structure. Reproduced from ref. 78 with permission.

4. Meshes, foams and microfibers as templating structures

There are other alternatives to the organic moulding using microspheres as is the use of any other type of organic-based materials. More specifically meshes, foams and microfibers have recently been proved to be an effective way to produce porosity with some specific pattern.^{81,82} The procedure is very simple and takes advantage of well-known techniques used in ceramic processing and SOFC technology such as is the use of tape-casting and dip-coating processes. First, a slurry containing the target powder material and some organic components is prepared. The composition of these slurries is based on typical tape-casting recipes.⁸³ The organic materials include: solvents, dispersants, binders and plasticisers. These components are ball-milled, typically for 1-2 h at 150-200 rpm.

Once the slurries have been prepared they can be used to impregnate any type of organic-based structure by dip-coating and left to dry at room temperature. After solvent evaporation, the coated material will be a flexible plastic-like material which can then be easily processed in different sizes and shapes, bended, rolled, twisted, etc. Finally, the organic components are removed by slow firing reaching temperatures ranging between 600-1400 °C for 2-4 h for desired metal oxide backbone formation, **Figs. 9-11**.

4.1. Polyester meshes

The use of polyester meshes allows the fabrication of a 2D/3D matrix of cross-linked channels through the whole SOFC electrode material.⁸¹ The size of the channels can be easily tailored ranging from a few microns up to hundreds of microns. The most remarkable feature is the stability of these structures up to 1500 °C, as well as the versatility of the method as it can be applied to any material commonly used in SOFC technology or in other fields, e.g. exhausts catalyst materials, biomaterials, storage materials, separation membranes, etc. The key element of the procedure is the use of a simple polyester mesh, **Fig. 9(a)**, as a template. Every single filament/wire of the initial mesh will be a potential channel in the final material, after burning off the mesh, **Fig. 9(c-f)**. The mesh is coated via dip-coating, using a slurry prepared with the target powder material. The thermoplasticity of the mesh allows it to be shaped in different morphologies by heating at 175 °C for 1 h, e.g. a flat piece of mesh can be transformed in a circular microtube, **Fig. 9(b)**. Other geometries such as hexagonal microtubes could be interesting for instance in the fabrication of SOFC stacks. In addition, the slurry of inorganic powders can be replaced for a dispersion of precious metal, and with the same methodology, some special configurations as Pt-hollow-meshes can be produced just after firing at 900 °C for 0.5 h. Given that the slurries are liquid then, the coated meshes can be covered by different slurries, with a perfect contact between layers in the green state. Also the contact between layers after firing at high temperature (1400 °C) remains in very good condition, **Fig. 9(d)**.

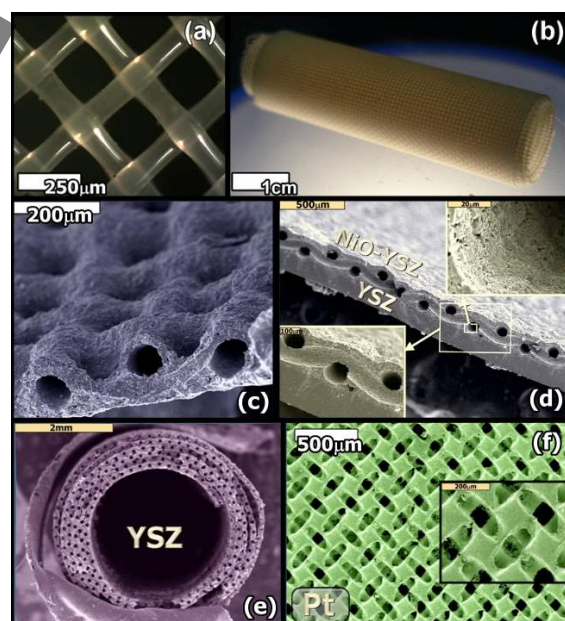


Fig. 9 (a) Polyester mesh used as template agent for the creation of a network of interconnected channels. (b) Polyester mesh shaped in circular microtube after heating at 175 °C for 1 h. (c) Channelled microstructure of NiO-YSZ composites, fired at 1400 °C for 5 h. (d) dense YSZ layer and a porous channelled layer of a composite of NiO-YSZ co-fired at 1400 °C for 5 h. (e) channelled YSZ-based microtubes of 4 mm wide. (f) Precious-metal hollow mesh (Pt in this case), fired at 900 °C for 0.5 h.⁸¹

This type of templating may facilitate the transport of fuel and oxidant gases to the reaction sites and provide easy removal of the gases produced from the corresponding electrochemical reactions. More specifically, it may solve the problems related to the fabrication of gas supplying channels within the bi-polar plates (in planar SOFC design).

4.2. NOMEXTM meshes

It is well-known that the honeycomb arrangement affords mechanical strength to any supported structure due to an effective distribution of the load.⁸⁴ Several materials with the aforementioned arrangement are commercially available, and among them, NOMEXTM mesh, Fig. 10(a). This material manufactured by DUPONTTM, is mainly made of meta-aramid fibers and exhibits several interesting properties, e.g. resistance to high temperatures. One may take advantage of this property to mould a ceramic-based material (e.g. YSZ) and create a backbone with hexagonal cells in a honeycomb structure. Zhong *et al.*⁸⁵ and Yamaguchi *et al.*⁸⁶ have also used the honeycomb configuration to produce alternative SOFC devices with promising performances.

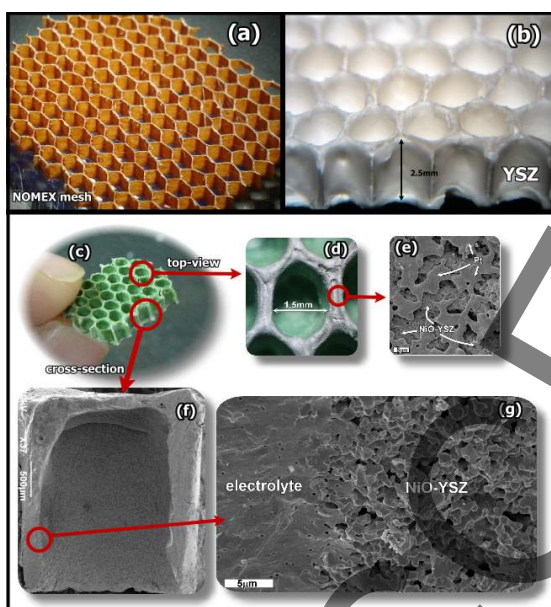


Fig. 10 (a) NOMEXTM honeycomb mesh with hexagonal cells used as templates. (b) Honeycomb YSZ-backbone moulded with NOMEXTM honeycomb mesh. (c) Assembled SOFC with honeycomb arrangement supporting a $\sim 100 \mu\text{m}$ thin YSZ layer. (d, e) Details of the edge of each cell painted with Pt paste and the porous structure of such layer. (f) Cross-section of an individual YSZ hexagonal cell. (g) Image showing the porous morphology of the NiO-YSZ composite in the inner part of each hexagonal cell. Reproduced from ref. 82.

In this novel design,⁸² a $\sim 100 \mu\text{m}$ -thick electrolyte layer is supported by a YSZ-honeycomb backbone with hexagonal cells. The honeycomb structure is covered with a thin layer (10-20 μm) of the active anode material which render performances of 320 mW cm^{-2} or 1.22 W cm^{-3} and OCV of 1.13 V, at $900 \text{ }^\circ\text{C}$, under humidified CH_4 .

The main feature is that the design may saves up to $\sim 70\%$ of the supporting material (electrolyte or electrode), which will eventually lead to a drastic decrease of the cost of any

stack assembled in this configuration. The main disadvantage is that the critical rupture tension was estimated to be 37.2 MPa.⁸² This value is rather low compared to the typical values of standard anode-supported SOFCs, i.e. 60-80 MPa, however it matches very well to the mechanical strength of very porous anode-supported cells, ($< 20 \text{ MPa}$).⁸⁷

The potential applications of this type of configuration include the possible fabrication of lighter SOFC devices with very high volumetric and/or gravimetric power densities.

Another potential application is the production of biofilter-supports for the degradation of organic volatile compounds (VOCs). YSZ-based honeycomb biofilters were fabricated and tested with several VOCs such as toluene, xylene and ethylbenzene, rendering performances of 80% for removing these contaminants. Hence the YSZ can be recovered from a SOFC that have reached the end of their lifetime and then a biofilter can be fabricated and used for VOCs removal with high efficiencies. Compared to traditional plastic filter, the YSZ-based filters can be regenerated after firing in oxidising conditions at $600 \text{ }^\circ\text{C}$ for few hours.

Other potential application of the honeycomb arrangement is as a support of specific catalysts for the production of biofuels. The main advantage with this approach is the production of a solid material that can be easily removed from the solution once the reaction has finished.

4.3. Polyurethane foams and microfibers

As already pointed out, any structure made of organic materials can be coated with an inorganic-based slurry. There are several interesting structures, maybe not for direct application in SOFC technology, such as foams, acrylic fibers, cotton, C-microfibers meshes, etc., Fig. 11.

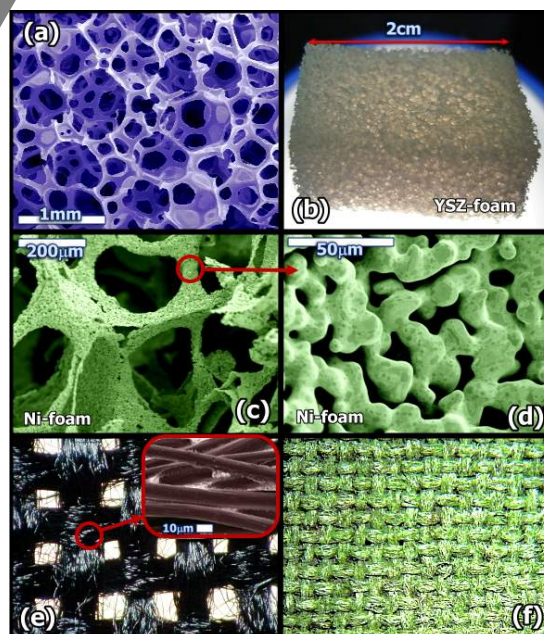


Fig. 11 (a) SEM image of polyurethane foam. (b) A YSZ-based replicated foam after firing at $1400 \text{ }^\circ\text{C}$ for 2 h. The structure remains highly porous (50-80%). (c, d) Ni-based foam after replicating with NiO-slurry, in oxidant conditions, and then firing under hydrogen at $800 \text{ }^\circ\text{C}$ for 5 h. (e) carbon-based microfibers ($\sim 8 \mu\text{m}$) can be replicated with any type

of inorganic materials, in this case (f) a composite of NiO-YSZ was produced at 1400 °C for 2h.

The foams⁵⁷ have several potential industrial applications and they can be easily impregnated with the ceramic-based slurry. After squeezing the coated structure to remove the excess of the deposited slurry, the sample is left to dry and the burning process produce replicated foam with a sintered material, Fig. 11(b). This type of procedure allows the fabrication of ceramic-based foams of zirconia, ceria-based materials, alumina or even the production of metal-based foams can be easily prepared through this route (Ni, Cu, etc.). For example, Ni foams find potential applications due to their excellent corrosion resistance and hardness. The procedure is similar to those mentioned above, the main difference being a final step in which the sample is reduced under a flow of 5% H₂/Ar, at 800 °C for 5 h. The foams produced, Fig. 11(c,d), can be used as: base plate of positive electrode in Ni-MH / Ni-Cd batteries, filtration materials of air/oil/smoke, porous electrode in Galvano-Chemistry engineering, heat dissipation, amortization materials, noise-absorbing and vibration-absorbing materials, electromagnetic shielding materials, catalyst carrier, precious metal recovery or just as current collector in the anode side of a SOFC.

5. Rubber-based moulds

In all the previous cases the organic-based moulding material (microspheres, meshes, foams, etc.) must be removed during the firing/sintering process. Recently Ruiz-Morales *et al.*⁸⁸ proposed an alternative approach where the moulding agent is a rubber-based material that can be used, at room temperature, to mould any tape of ceramic-based material, Fig. 12. This mould can be easily peeled-off from the moulded ceramic, at room temperature, without using any releasing agent and thus the mould can be reused several times helping to reduce costs in a possible application of this procedure at commercial scale.

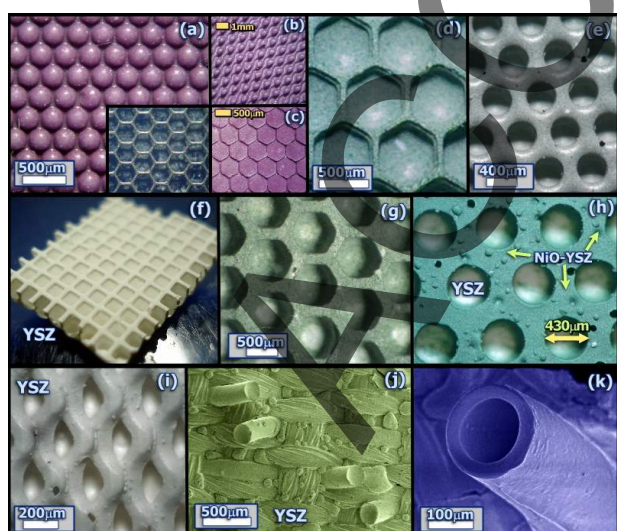


Fig. 12 (a,b,c) Rubber moulds with different patterning - inset of (a) show details of a metallic mesh used to transfer the patterning to the mould at room temperature. (d, e) Moulded materials in the green state after peel-off from the moulds, NiO-YSZ (d) without and (e) with glassy carbon

microspheres (as pore former). (f, i) moulded YSZ backbone after firing at 1400 °C for 2 h. (g, h) moulded structures with honeycomb backbone arrangement of a NiO-YSZ SOFC anode with (g) hexagonal cells or (h) circular cells, both supporting a thin layer of YSZ. The structures were co-fired at 1400 °C for 2 h. (j,k) Any type of details, ranging from a few microns to hundred of microns can be simultaneously replicated. (k) YSZ layers covered with YSZ microtubes can be also produced.⁸⁸

The specific pattern to be moulded is obtained using metallic meshes with the desired pattern, -inset of Fig. 12(a)-. This pattern can be transferred in just 20 minutes to a two-component rubber-based material. Pressing together the metallic mesh with the rubber in the green state allows, after the curing at room temperature, to obtain a mould with some specific pattern, Fig. 12 (a,b,c).

Once the mould has been cured, it can be filled with a slurry of the material to be moulded. After the solvent evaporation two plastic-based materials are obtained: the rubber-mould and the moulded inorganic material. Because of that, the flexibility of both elements allows to easily peel-off the moulded material, Fig. 12 (d,e). These moulded materials remain very flexible and they can be easily manipulated as required (cut, bended, rolled, etc.). The final step is a firing process at 1200-1400 °C for 2-4 h which renders perfect replicated structures with precisely controlled features such as: size and distribution of the pore holes in the structure, the thickness of the electrode and electrolyte layers, type of patterning, etc., Fig. 12 (f-k).

The main disadvantage is related to the materials co-firing step. In that case bending problems can arise. Features ranging between 50 μm (walls of the honeycomb cells) and 500 μm (size of honeycomb cells) have been replicated using this method. Typically this route allows fabricating details in the range of 200-300 μm but new modifications in the procedure allow replicating details of a few microns, Fig. 12(j). This type of structure is ideal to produce rough surfaces that allow facile attachment of the electrode material. Also the incorporation of YSZ microtubes, Fig. 12 (j,k), allows increasing the available contact area and hence potentially boosting the performance of any SOFC assembled with electrolytes moulded with this type of surface.

As a future direction in this type of moulding, the most attractive option is going down to the sub-micrometer and nanometer range. The production of moulds in that scale can be achieved through the use of photolithography.^{89,90}

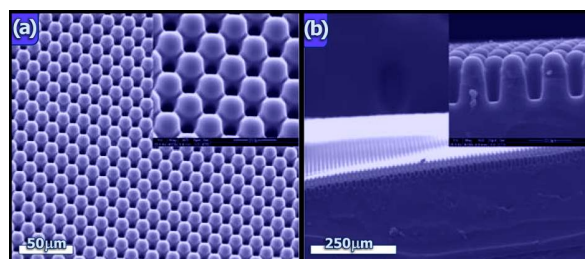


Fig. 13 (a,b) SEM images showing details of structure fabricated in PDMS by photolithography. Reproduced from ref. 89 with permission.

This technique is regularly used to control precisely small details in a large number of microdevices such as microelectronic circuits, microelectromechanical systems,

microfluidic devices, and nucleic acid-protein microarrays,⁹¹ but it has been scarcely applied to control materials for SOFC applications at high temperatures.⁹² Basically it consists in illuminating selectively a thin photosensitive resin with UV light through a mask containing opaque features on a transparent background (e.g. glass or plastic). After a development process, the UV resin will reveal a patterned area that can be now replicated with a polymeric material such as poly(dimethylsiloxane) (PDMS). PDMS will be the equivalent to our rubber-based mould but rendering details of few micrometers, Fig. 13.

6. Glassy carbon microspheres

All the previously commented routes were developed, mainly, for moulding inorganic materials. However we have been able to apply the same methodology to powder of just glassy carbon microspheres (GCMs).⁹³ This material exhibits a high resistance to the decomposition in reducing conditions, e.g. it can reach temperatures superior to 2000 °C without decomposition, and is stable in acid and basic media. The microspheres also show high hardness, low density and low thermal expansion, biocompatibility and good electrical conductivity. Therefore, the production of structures made of GCMs to take advantage of all these properties in several technological areas may be considered relevant. Hence, apart from using GCMs just as a pores former material, the approach opens up the possibility to create macrostructures just made out of GCMs such as meshes, microfibers or foams,⁹³ Fig.14.

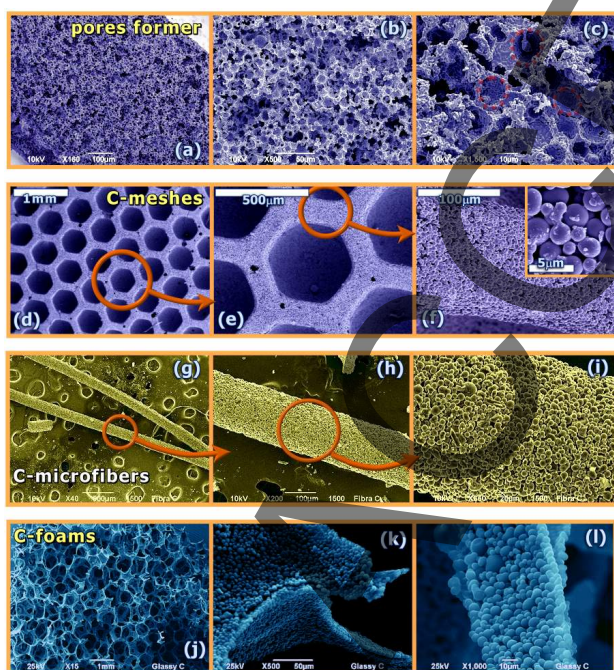


Fig. 14 (a-c) GCMs is used as pores former for the fabrication of porous YSZ-based membranes at 1400 °C for 2 h. **(d-f)** GCMs-based meshes, mean size of GCMs ~5 μm. **(g-i)** GCMs-based microfibers prepared by extrusion. **(j-l)** GCMs-based foams, fired at 300 °C for 2 h. Reproduced from ref 93.

The structures similar to those described in sections 4-5 can

be prepared with GCMs. This is achieved by just replacing the inorganic material for GCMs in the slurry recipe. The slurry can be used to fill rubber-based moulds and hence to produce different arrangements, Fig. 14 (d-f). Furthermore, the slurry can be extruded through a micrometer-sized needle to GCMs-based microfibers, Fig. 14 (g-i) or it can be used to dip-coat polyurethane foams to produce GCMs-based foams, Fig. 14 (j-l). In all the cases, the GCMs structures remain flexible at room temperature. Then they can be fired at 175 °C for 1-2 h to produce a rigid structure that remains porous. In the case of the foams a temperature of 300 °C is used to remove the polyurethane base mould. Porosity ranging between 30-75% has been obtained.⁹³ Hence, these structures remain porous and they can still be used as pore formers in a porous mould, catalyst-supports, templating agents to mould inorganic-based materials, or they can be used as current-collectors/electrodes in several fields, though mainly related to Energy as is the case of fuel cells electrodes.

For example, GCMs meshes have been infiltrated with an acid solution of tetraethoxysilane (TEOS) allowing the condensation around the GCMs. After firing at 650 °C for 5 h, the GCMs backbone is removed leaving a mesh of hollow-SiO₂ microspheres with mesoporosity (~7 nm), BET values of 40 m²/g and a very light structure with 91% of porosity.⁹³

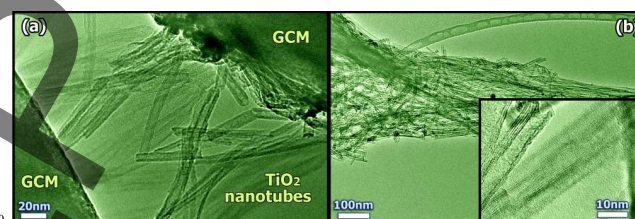


Fig. 15 (a-b) TiO₂-based nanotubes growth over the surface of GCMs, at 140 °C for 20 h.

Other potential applications come from the possibility to control the arrangement of a photocatalyst material such as TiO₂, that typically is used to destroy organic pollutants.^{94,95} We have been able to promote the growth of TiO₂-based-nanotubes on the surface of GCMs, at 140 °C, Fig. 15. Providing GCMs-based structures as meshes, foams or microfibers containing TiO₂-nanotubes that are easier to manipulate than the nanotubes themselves.

7. Membrane-based templates for the fabrication of nanotubes

In the previous method, the surface of a specific material was used to promote the growth of inorganic-based nanotubes, but still quite difficult to obtain an ordered distribution of them. For this purpose a membrane can be used as a templating agent. The holes in the membrane will control the direction of the growth of the nanotubes. One can choose between organic- or inorganic-based membranes. After the templating procedure, the organic membrane material will be removed by a thermal treatment whereas the inorganic membranes commonly are removed by a chemical procedure.

Levy *et al.*⁹⁶ used organic polycarbonate films to fabricate nanotubes of simple or complex oxides. This procedure has

been successfully applied for the fabrication of SOFC cathodes materials such as $\text{La}_{0.6}\text{Sr}_{0.4}\text{CoO}_3$ (LSCO), Fig.16.⁹⁷

Some issues are related with the direct attachment of the nanotubes to the electrolyte and hence a specific ink need to be used for this purpose.⁹⁷ The final temperature must be higher enough to properly attach the nanotubes to the electrolyte and lower enough to avoid an excessive agglomeration of the nanoparticles destroying the ordered structures.

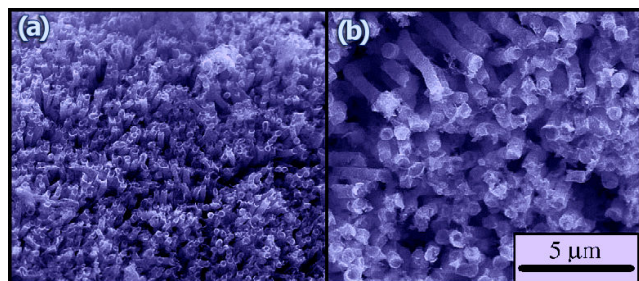


Fig. 16 (a-b) LSCO nanotubes prepared from polycarbonate-based Millipore™ membranes, before final firing process. Reproduced from ref. 97 with permission.

In the other hand, the use of an inorganic-based membrane, was recently proposed to assist in the fabrication of CeO_2/Ni concentric nanostuctures.⁹⁸ In this approach, a nanoporous anodized aluminium oxide (AAO) membrane is used as template, Fig. 17. A Ti-layer was deposited as an electrical contact and then ceria-based nanotubes are deposited by electrodeposition in the AAO nanopores. After removing the AAO template in a basic solution, Ni is electrodeposited replicating the original AAO template and hence embedding the matrix of ceria nanotubes, Fig 17 (a,b). Modifying the experimental conditions coaxial nanotubes of Ni-CeO_2 can be produced, Fig. 17 (c). This type of configuration can be promising in enhancing the performance of SOFC anodes, given than it provides TPB areas 30 times higher than that of typical anode structures.⁹⁸

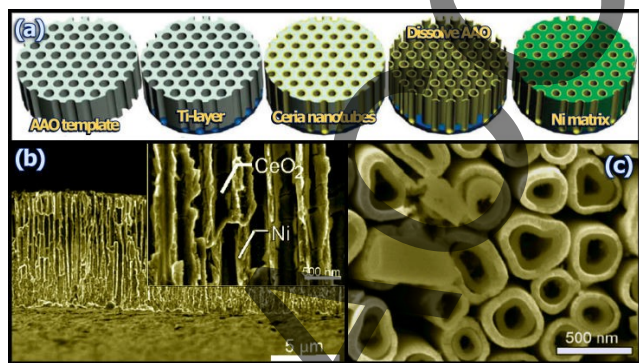


Fig. 17 (a) Scheme showing the fabrication of a film of Ni with an embedded matrix of ceria nanotubes. (b) SEM image of the cross-section of a Ni-CeO_2 film. (c) top-view of a coaxial arrangement of Ni-CeO_2 nanotubes.⁹⁸ Reproduced by permission of the PCCP Owner Societies.

Conclusions

Several cost-effective methods to control the microstructure of the materials for SOFC applications have been explored. These methods allow the replication of virtually any type of

patterned details ranging from “eye-scale” down to the micrometer scale. It has been shown that the porosity can be tailored depending on the specific application envisaged by the end user. The main advantage is the versatility of the proposed approaches, which makes them interesting not only for SOFC but for a wide range of energy and environmental applications.

Even though these methods are really cost-effective another parameter that should be always kept on mind is the time consumed in the fabrication of any type of structure. Normally 2 or 3 days can be required for the deposition of several layers of different materials, drying process/solvent evaporation, electrodeposition, carefully control of the patterning, etc. And hence all these processes are in disadvantage compared with the traditional SOFC method of mixing inorganic powder plus organic pore formers and just fire the mixture. The reduction of the fabrication time in any of the aforementioned procedures will boost it changes to become a standard in the control of microstructures.

Notes and references

- ^a Dpto. Química Inorgánica, Universidad de La Laguna, Avda. Astrofísico Francisco Sánchez s/n, CP: 38200, Tenerife, Spain. E-mail: jcrui@ull.es
^b Dpto. de Física Aplicada I, Universidad de Málaga, 29071-Málaga, Spain.
^c Instituto de Energías Renovables, Parque Científico y Tecnológico de Albacete, Universidad de Castilla la Mancha, 02006-Albacete, Spain.
^d School of Chemistry, University of St Andrews, North Haugh, KY16 9ST, St Andrews, Scotland, UK.

- 1 N. Q. Minh and T. Takahashi, in *Science and Technology of Ceramic Fuel Cells*, Elsevier, Amsterdam (The Netherlands), 1995.
- 2 B. C. H. Steele, *J. Mater. Sci.*, 2001, **36**, 1053-1068.
- 3 A. Orera and P. R. Slater, *Chem. Mater.*, 2010, **22**, 675-690.
- 4 A. S. Aricò, P. Bruce, B. Scrosati, J.-M. Tarascon and W. van Schalkwijk, *Nat. Mater.*, 2005, **4**, 366-377.
- 5 S. Mitragotri and J. Lahann, *Nat. Mater.*, 2008, **8**, 15-23.
- 6 A. Barona, A. Elias, I. Cano, A. Uriarte and J. Artetxe, *Chem. Biochem. Eng. Q.*, 2007, **21**, 151-157.
- 7 A. Brito, M. E. Borges, M. Garín and A. Hernández, *Energy Fuels*, 2009, **23**, 2952-58.
- 8 J. C. Ruiz-Morales, J. Canales-Vázquez, C. Savaniu, D. Marrero-López, W. Zhou and John T. S. Irvine, *Nature*, 2006, **439**, 568-571.
- 9 T. Suzuki, Z. Hasan, Y. Funahashi, T. Yamaguchi, Y. Fujishiro and M. Awano, *Science*, 2009, **325**, 852-855.
- 10 F. Zhao and A. V. Virkar, *J. Power Sources*, 2005, **141**, 79-95.
- 11 L. Hu, S. Dai, J. Weng, S. Xiao, Y. Sui, Y. Huang, S. Chen, F. Kong, X. Pan, L. Liang and K. Wang, *J. Phys. Chem. B*, 2007, **111**, 358-362.
- 12 M. E. Borges, M. C. Alvarez-Galván, P. Esparza, E. Medina, P. Martín-Zarza and J. L. G. Fierro, *Energy Environ. Sci.*, 2008, **1**, 364-369.
- 13 J. C.-S. Wu and L.-C. Cheng, *J. Membr. Sci.*, 2000, **167**, 253-261.
- 14 L. Schlupbach and A. Züttel, *Nature*, 2001, **414**, 353-358.
- 15 M. J. Ledoux and C. Pham-Huu, *CATTECH*, 2001, **5**, 226-246.
- 16 J. Kašpar, P. Fornasiero and N. Hickey, *Catal. Today*, 2003, **77**, 419-449.
- 17 D. Tonti, M. J. Torralvo, E. Enciso, I. Sobrados and J. Sanz, *Chem. Mater.*, 2008, **20**, 4783-4790.
- 18 T. Kudo and H. Obayashi, *J. Electrochem. Soc.*, 1976, **123**, 415-419.
- 19 M. Mogensen, N. M. Sammes and G. A. Tompsett, *Solid State Ionics*, 2000, **129**, 63-94.
- 20 P. Lacorre, F. Goutenoire, O. Bohnke, R. Retoux and Y. Laligant, *Nature*, 2000, **404**, 856-858.

- 21 D. Marrero-López, J. Peña-Martínez, J. C. Ruiz-Morales, D. Pérez-Coll, M. C. Martín-Sedeño and P. Núñez, *Solid State Ionics*, 2007, **178**, 1366-1378.
- 22 D. Marrero-López, J. Canales-Vázquez, J. C. Ruiz-Morales, John T. S. Irvine and P. Núñez, *Electrochim. Acta*, 2005, **50**, 4385-4395.
- 23 T. Ishihara, H. Matsuda and Y. Takita, *J. Am. Chem. Soc.*, 1994, **116**, 3801-3803.
- 24 S. Nakayama, T. Kageyama, H. Aono and Y. Sadaoka, *J. Mater. Chem.*, 1995, **5**, 1801-1805.
- 25 D. Marrero-López, M. C. Martín-Sedeño, J. Peña-Martínez, J. C. Ruiz-Morales, P. Núñez, M. A. G. Aranda, J. R. Ramos-Barrado, *J. Power Sources*, 2010, **195**, 2496-2506.
- 26 J. E. H. Sansom, D. Richings and P. R. Slater, *Solid State Ionics*, 2001, **139**, 205-210.
- 27 P. R. Slater, J. E. H. Sansom and J. R. Tolchard, *Chem. Rec.*, 2004, **4**, 373-384.
- 28 R. J. Gorte, S. Park, J. M. Vohs and C. Wang, *Adv. Mater.*, 2000, **12**, 1465-1469.
- 29 S. Park, J. M. Vohs and R. J. Gorte, *Nature*, 2000, **404**, 265-267.
- 30 S. W. Tao and John T. S. Irvine, *Nat. Mater.*, 2003, **2**, 320-323.
- 31 S. W. Tao and John T. S. Irvine, *J. Electrochem. Soc.*, 2004, **151**, A252-A259.
- 32 J. Canales-Vázquez, S. W. Tao and John T. S. Irvine, *Solid State Ionics*, 2003, **159**, 159-165.
- 33 J. Canales-Vázquez, J. C. Ruiz-Morales, John T. S. Irvine and W. Zhou, *J. Electrochem. Soc.*, 2005, **152**, A1458-A1465.
- 34 A. Ovalle, J. C. Ruiz-Morales, J. Canales-Vázquez, D. Marrero-López and John T. S. Irvine, *Solid State Ionics*, 2006, **117**, 1997-2003.
- 35 J. C. Ruiz-Morales, J. Canales-Vázquez, C. Savaniu, D. Marrero-López, P. Núñez, W. Zhou and John T. S. Irvine, *Phys. Chem. Chem. Phys.*, 2007, **9**, 1821-1830.
- 36 Y. H. Huang, R. I. Dass, Z. L. Xing and John B. Goodenough, *Science*, 2006, **312**, 254-257.
- 37 D. Marrero-López, J. Peña-Martínez, J. C. Ruiz-Morales, D. Pérez-Coll, M. G. A. Aranda and P. Núñez, *Mater. Res. Bull.*, 2008, **43**, 2441-2450.
- 38 O. A. Marina, N. L. Canfield and J. W. Stevenson, *Solid State Ionics*, 2002, **149**, 21-28.
- 39 L. Yang, S. Wang, K. Blinn, M. Liu, Z. Cheng and M. Liu, *Science*, 2009, **326**, 126-129.
- 40 R. Mukundan, E. L. Brosha and F. H. Garzon, *Electrochem. Solid-State Lett.*, 2004, **7**, A5-A7.
- 41 J. Canales-Vázquez, M. J. Smith, J. T. S. Irvine and W. Zhou, *Adv. Funct. Mater.*, 2005, **15**, 1000-1008.
- 42 M.-C. Zhan, W.-D. Wang, T.-F. Tian and C.-S. Chen, *Energy Fuels*, 2010, **24**, 764-771.
- 43 J. M. Fox III, *Catal. Rev. -Sci. Eng.*, 1993, **35**, 169-212.
- 44 Z. Shao and S. M. Haile, *Nature*, 2004, **431**, 170-173.
- 45 V. V. Kharton, E. V. Tsipis, A. A. Yaremchenko, I. P. Marozau, A. P. Viskup, J. R. Frade and E. N. Naumovich, *Mat. Sci. Eng., B*, 2006, **134**, 80-88.
- 46 H. Y. Tu, Y. Takeda, N. Imanishi and O. Yamamoto, *Solid State Ionics*, 1997, **100**, 283-288.
- 47 H. Ullmann, N. Trofimenko, F. Tietz, D. Stöver and A. Ahmad-Khanlou, *Solid State Ionics*, 2000, **138**, 79-90.
- 48 C. N. Munnings, S. J. Skinner, G. Amow, P. S. Whitfield and I. J. Davidson, *Solid State Ionics*, 2005, **176**, 1895-1901.
- 49 E. Boehm, J.-M. Bassat, P. Dordor, F. Mauvy, J.-C. Grenier and Ph. Stevens, *Solid State Ionics*, 2005, **176**, 2717-2725.
- 50 S. J. Skinner and J. A. Kilner, *Solid State Ionics*, 2000, **135**, 709-712.
- 51 J. M. Ralph, A. C. Schoeler and M. Krumpelt, *J. Mater. Sci.*, 2001, **36**, 1161-1172.
- 52 A. Tarancón, S. J. Skinner, R. J. Chater, F. Hernández-Ramírez and J. A. Kilner, *J. Mater. Chem.*, 2007, **17**, 3175-3181.
- 53 G. Kim, S. Wang, A. J. Jacobson, L. Reimus, P. Brodersen and C. A. Mims, *J. Mater. Chem.*, 2007, **17**, 2500-2505.
- 54 A. Tarancón, A. Morata, G. Dezanneau, S. J. Skinner, J. A. Kilner, S. Estrade, F. Hernández-Ramírez, F. Peiró and J. R. Morante, *J. Power Sources*, 2007, **174**, 255-263.
- 55 A. Tarancón, J. Peña-Martínez, D. Marrero-López, A. Morata, J. C. Ruiz-Morales and P. Núñez, *Solid State Ionics*, 2008, **179**, 2372-2378.
- 56 Y. Zhang, S. Zha and M. Liu, *Adv. Mater.*, 2005, **17**, 487-491.
- 57 A. R. Studart, U. T. Gonzenbach, E. Tervoort and L. J. Gauckler, *J. Am. Ceram. Soc.*, 2006, **89**, 1771-1789.
- 58 S. P. Jiang, *Mat. Sci. Eng., A*, 2006, **418**, 199-210.
- 59 R. Chiba, F. Yoshimura, Y. Sakurai, Y. Tabata and M. Arakawa, *Solid State Ionics*, 2004, **175**, 23-27.
- 60 X. Xu, Z. Jiang, X. Fan and C. Xia, *Solid State Ionics*, 2006, **177**, 2113-2117.
- 61 J. Chen, F. Liang, L. Liu, S. Jiang, B. Chi, J. Pu and J. Li, *J. Power Sources*, 2008, **183**, 586-589.
- 62 S. Boullfrad, M. Cassidy and John T. S. Irvine, *Adv. Funct. Mater.*, 2010, **20**, 861-866.
- 63 F. Liang, J. Chen, S. P. Jiang, B. Chi, J. Pu and L. Lian, *Electrochem. Commun.*, 2009, **11**, 1048-1051.
- 64 J. C. Ruiz-Morales, J. Canales-Vázquez, J. Peña-Martínez, D. Marrero-López, John T. S. Irvine and P. Núñez, *J. Mater. Chem.*, 2006, **16**, 540-542.
- 65 D. Zou, S. Ma, R. Guan, M. Park, L. Sun, J. J. Aklonis, R. Salovey, *J. Polym. Sci., Part A: Polym. Chem.*, 1992, **30**, 137-144.
- 66 C. Savaniu and John T. S. Irvine, *J. Mater. Chem.*, 2009, **19**, 8119-8128.
- 67 E. C. Brown, S. K. Wilke, D. A. Boyd, D. G. Goodwin and S. M. Haile, *J. Mater. Chem.*, 2010, **20**, 2190-2196.
- 68 O. D. Velev, T. A. Jede, R. F. Lobo and A. M. Lenhoff, *Nature*, 1997, **389**, 447-448.
- 69 O. D. Velev and A. M. Lenhoff, *Curr. Opin. Colloid Interface Sci.*, 2000, **5**, 56-63.
- 70 S. Wong, V. Kitaev and G. A. Ozin, *J. Am. Chem. Soc.*, 2003, **125**, 15589-15598.
- 71 R. C. Schroden and A. Stein, "3D Ordered Macroporous Material", In *Colloids and Colloid Assemblies*, Ed. F. Caruso, Wiley-VCH, Weinheim, Germany, 2004, **465-493**.
- 72 A. Stein, *Microporous Mesoporous Mater.*, 2001, **44**, 227-239.
- 73 A. Stein and R. C. Schroden, *Curr. Opin. Solid State Mater. Sci.*, 2001, **5**, 553-564.
- 74 M. C. Carbajo, A. Gomez, M. J. Torralvo and E. Enciso, *J. Mater. Chem.*, 2002, **12**, 2740-2746.
- 75 M. Sadakane, T. Asanuma, J. Kubo and W. Ueda, *Chem. Mater.*, 2005, **17**, 3546-3551.
- 76 H. Yan, C. F. Blandford, B. T. Holland, W. H. Smyrl and A. Stein, *Chem. Mater.*, 2000, **12**, 1134-1141.
- 77 D. Marrero-López, J. C. Ruiz-Morales, J. Peña-Martínez, J. Canales-Vázquez and P. Núñez, *J. Solid State Chem.*, 2008, **181**, 685-692.
- 78 A. Lashtabeg, J. Drennan, R. Knibbe, J. L. Bradley and G. Q. Lu, *Microporous Mesoporous Mater.*, 2009, **117**, 395-401.
- 79 A. Lashtabeg, J. L. Bradley, G. Vives, J. Drennan, *Ceram. Int.*, 2010, **36**, 653-659.
- 80 Y. An, S. J. Skinner and D. W. McComb, *J. Mater. Chem.*, 2010, **20**, 248-254.
- 81 J. C. Ruiz-Morales, J. Peña-Martínez, J. Canales-Vázquez, D. Marrero-López, C. Savaniu and P. Núñez, *J. Am. Ceram. Soc.*, 2009, **92**, 276-279.
- 82 J. C. Ruiz-Morales, D. Marrero-López, J. Peña-Martínez, J. Canales-Vázquez, J. J. Roa, M. Segarra, S. N. Savvin and P. Nunez, *J. Power Sources*, 2010, **195**, 516-521.
- 83 R. E. Mistler and E. R. Twiname, In *Tape Casting: Theory and Practise*, Wiley-American Ceramic Society, Westerville, OH, 2000.
- 84 C. C. Foo, G. B. Chai and L. K. Seah, *Compos. Struct.*, 2007, **80**, 588-594.
- 85 H. Zhong, H. Matsumoto, T. Ishihara and A. Toriyama, *Solid State Ionics*, 2008, **179**, 1474-1477.
- 86 T. Yamaguchi, S. Shimizu, T. Suzuki, Y. Fujishiro and M. Awano, *J. Am. Ceram. Soc.*, 2009, **92**, S107-S111.
- 87 M. Radovic, and E. Lara-Curzio, *Acta Mater.*, 2004, **52**, 5747-5756.
- 88 J. C. Ruiz-Morales, D. Marrero-López, J. Canales-Vázquez, P. Núñez and J. M. Domínguez-González, *Fuel Cells*, 2010, doi: 10.1002/fuce.201000035

-
- 89 C. T. Lim, H. Y. Low, J. K. K. Ng, W.-T. Liu and Y. Zhang, *Microfluid. Nanofluid.*, 2009, **7**, 721-726.
- 90 X.-J. Huang, D.-H. Kim, M. Im, J. H. Lee, J.-B. Yoon and Y.-K. Choi, *Small*, 2009, **5**, 90-94.
- 5 91 M. J. Madou, In *Fundamentals of Microfabrication*, CRC Press, Boca Raton, FL, 1997.
- 92 E. Koep, C. Compson, M. Liu and Z. Zhou, *Solid State Ionics*, 2005, **176**, 1-8.
- 93 J. C. Ruiz-Morales, J. Canales-Vázquez, D. Marrero-López, S. N. Savvin, A. Dos Santos, C. Sánchez-Bautista and J. Peña-Martínez, *Carbon*, 2010 (accepted), doi 10.1016/j.carbon.2010.06.012
- 10 94 J. Araña, J. M. Doña-Rodríguez, E. Tello Rendón, C. Garriga i Cabo, O. González-Díaz, J. A. Herrera-Melián, J. Pérez-Peña, G. Colón and J. A. Navío, *Appl. Catal., B*, 2003, **44**, 161-172.
- 15 95 M. Alam Khan, H.-T. Jung and O.-B. Yang, *J. Phys. Chem. B.*, 2006, **110**, 6626-6630.
- 96 P. Levy, A. G. Leyva, H. E. Troiani, R. D. Sánchez, *Appl. Phys. Lett.*, 2003, **83**, 5247-5249.
- 97 J. Sacanell, A. G. Leyva, M. G. Bellino, D. G. Lamas, *J. Power Sources*, 2010, **195**, 1786-1792.
- 20 98 C. Zhang, J. Grandner, R. Liu, S. B. Lee and B. W. Eichhorn, *Phys. Chem. Chem. Phys.*, 2010, **12**, 4295-4300.

ACCEPTED